# Transformer Neural Network for Early Battery Capacity Prediction Based on Electrochemical Impedance Spectroscopy


Zhansheng Ning
*PE group, Faculty EEMCS*
*University of Twente*
Enschede, The Netherlands
z.ning@utwente.nl

Prasanth Venugopal
*PE group, Faculty EEMCS*
*University of Twente*
Enschede, The Netherlands
prasanth.venugopal@utwente.nl

Gert Rietveld
*PE group, Faculty EEMCS*
*University of Twente*
Enschede, The Netherlands
g.rietveld@utwente.nl
*and VSL, Delft, The Netherlands*

Thiago Batista Soeiro
*PE group, Faculty EEMCS*
*University of Twente*
Enschede, The Netherlands
t.batistasoeiro@utwente.nl



***Abstract*—Early prediction of the decaying capacity of lithium-ion batteries is significant for *e.g.* early detection of abnormal cells in a battery pack. Due to the influence of the historical aging path on battery health, traditional battery capacity prediction methods rely on a large dataset of measured capacity data, which make them unsuitable for early battery capacity prediction and real-time application. To improve this situation, a multivariate and direct multi-step prediction transformer model based on electrochemical impedance spectroscopy (EIS) is proposed. To allow for real-time application, first, a robust battery capacity estimator is trained by using a convolution neural network based on EIS. Subsequently, by using the estimated capacity and impedance data, the proposed transformer model is trained for capacity prediction. Compared with five baseline models and published models, the proposed model has the best performance with prediction errors that are reduced by around 30 %. Compared with five published methods, the proposed model can indeed achieve earlier capacity prediction: only 5 cycles of data are needed for making a 15 cycle capacity prediction.**



***Index Terms*—Lithium-ion battery, Capacity estimator, Capacity prediction, Transformer, Direct multi-step prediction, EIS**


## I. Introduction

The rapid development of lithium-ion battery technology has led to the massive deployment of electric vehicles and furthermore stimulates electrification of ships [1]. However, many technical challenges relating to batteries are still unsolved, such as early warning of battery failure, early abnormal cell detection, and evaluation of battery health status, which all heavily depend on the capability for early prediction of decaying battery capacity. For reliable and efficient battery use, there is an urgent need to develop early capacity prediction techniques for advanced battery management systems [2].

The aging of batteries is nonlinear and is significantly affected by temperature, current rate, depth of discharge, chemistry, and manufacturing process, which leads to very different aging behavior of the battery. This makes it very challenging to establish a stable mapping relationship between battery capacity and for example cycle number, attracting many researchers to work on solving this challenge [3].

In recent years, data-driven methods have attracted more and more attention from academia and industry. Since capacity is affected by historical aging paths, capacity prediction can be considered a time series problem. Many iterative multi-step models are developed needing more than 60% of the full measured capacity dataset for adequate training and thus only can predict a narrow range of capacity values [4]. Another major disadvantage of these models is that it depends on the measured capacity, which makes it inappropriate in real applications because there is no opportunity to measure the actual capacity value after each cycle [5]. Finally, this method only considers specific battery cells to train the model, which makes the application to other cells unreliable [6]. Some researchers have developed multivariate capacity prediction models considering temperature, current, and voltage. This input information is often strongly related to battery aging, which indeed may improve the accuracy and robustness of models based on this type of data. However, the methods are usually based on direct multi-step capacity prediction, which again leads to a narrow prediction window [7]. The key approach to improve the prediction window is to use advanced networks with the ability of long output sequences.

The long short-term memory (LSTM) recurrent neural network (RNN) is a mature method for time series prediction, but still has difficulties in dealing with long sequences [6]. The transformer neural network stands out as one of the most successful sequence modeling architectures, showcasing unmatched performance across diverse applications, particularly in the fields of natural language processing and computer vision [8]. The transformer effectively captures long-range dependencies, thanks to the multi-head self-attention mechanism's efficacy. However, the suitability of transformer neural networks for time series prediction still needs further study. Some data sets, including traffic, electricity, weather, have already been used to explore the effectiveness of transformer models. Lithium-ion battery data is required to verify the effectiveness of the transformer in processing long input sequences [9].


2023 IEEE International Conference on Metrology for eXtended Reality, Artificial Intelligence and Neural Engineering (MetroXRAINE) | 979-8-3503-0080-2/23/$31.00 ©2023 IEEE | DOI: 10.1109/METROXRAINE58569.2023.10405626

To bridge this research gap, this paper proposes a multivariate and direct multi-step transformer neural network model based on electrochemical impedance spectroscopy (EIS). The main contributions of this article include the following:

1) The impedance of EIS data is considered as input variable of the transformer model, which helps improving capacity prediction accuracy.
2) Compared to the LSTM-RNN technique for capacity prediction, the transformer model is less affected by the length of the input and output sequence.
3) The use of a direct multi-step prediction architecture can improve the capacity prediction robustness compared with an iterative multi-step prediction architecture.

## II. Battery Data Set

The data set used in this article includes EIS and capacity data of 8 $LiCoO_2$/graphite cells, all obtained from [10]. The nominal capacity of the cells is 45 mAh and all 8 cells (named 25C01-25C08) are cycled with 1C CC charging and 2C CC discharging, at a test temperature of 25 °C. To avoid the influence of temperature, SOC and relaxation time on EIS, 25 °C, 100 % SOC, and 15 minutes resting time are set as the standard condition for the EIS measurements. The real part and imaginary part impedance are determined at 60 different frequencies selected from the frequency range of 0.02 Hz - 20 kHz. The EIS curves for fresh and aged cells of cell 01, cell 02, cell 03, and cell 06 are shown in Fig. 1 (a). Fig. 1 (b) gives the capacity declining curves for the 8 cells.

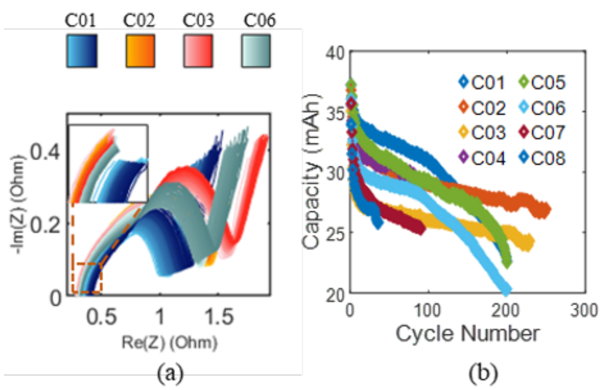


Fig. 1. Battery data set used in this study [10]. (a) EIS measurement result, the color changes from light to dark as the battery degrades. (b) Aging rate of 8 cells.

## III. Battery Capacity Prediction Methodology

A multivariate and direct multi-step prediction transformer model is proposed at method for predicting battery capacity and five baseline models are used to verify the effectiveness of the proposed model.

### *A. Multivariate and direct multi-step prediction transformer model*

The battery capacity prediction is a time series and it is realized by the early capacity sequence and features data, which is a typical time sequence prediction problem. The proposed framework of battery capacity prediction is shown in Fig. 2, including an encoder and a decoder. The encoder handles large, lengthy sequence inputs and compresses them into a concatenated feature map. On the other hand, the decoder receives extended sequence inputs without labels, calculates the weighted attention composition of the feature map, and generates the final predicted sequence [8]. The encoder and decoder are commonly implemented using LSTM-RNN, however, this limits the input and prediction length in direct multi-step prediction applications, considering the ability to capture long-dependencies, the transformer is used to construct the encoder and decoder.

The input and output sequences of the proposed model are formed as,

$$D = [input|output] = \left(\begin{array}{cc|c} c_1 & z_1 & c_{n+1} \\ c_2 & z_2 & c_{n+2} \\ \vdots & \vdots & \vdots \\ c_n & z_n & c_{n+p} \end{array}\right) \quad (1)$$

where $c$ is the capacity sequence, $z$ is the impedance sequence, where the imaginary part of impedance at the frequency of 2 Hz is used, because the frequency of 2HZ has the strongest correlation with battery capacity [10], $n$ is the length of input sequence, and $p$ is the length of the prediction sequence.

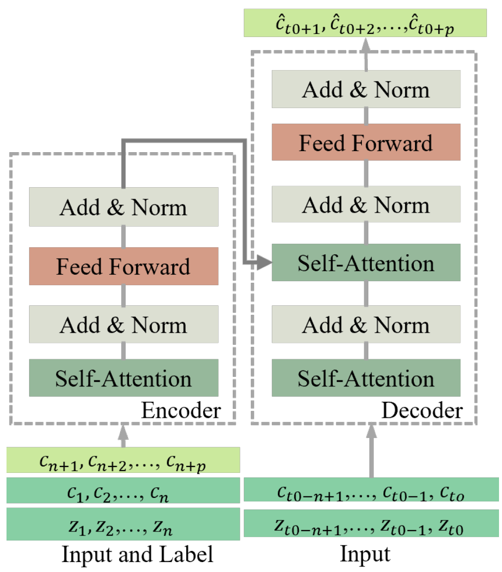


Fig. 2. Transformer architecture for battery capacity prediction. $c$ is the capacity sequence, $z$ is the imaginary part of the impedance of EIS data at a frequency of 2 Hz, $t_0 + 1$ is the capacity prediction start point, $n$ is the input length, $p$ is the direct multi-step prediction length, and $\hat{c}$ is the predicted capacity.

### *B. Baseline models*

Battery capacity prediction based on data-driven approaches can be divided into different categories according to the number of input variables, sequence prediction neural network, and prediction architecture. Five different combination methods are introduced as baseline models.

*a) Input variables:* In order to establish a data-driven method to accurately predict the battery capacity, features highly related to battery capacity need to be used as the input variables. According to the number of the input variables, there are two categories prediction models, which are multivariate and univariate prediction model.

*b) Sequence prediction method:* Long sequence time-series prediction demands a high prediction model, which is a model with the ability to capture precise long-range dependency coupling between output and input efficiently. Compared with LSTM-RNN models, transformer models have shown superior performance in capturing long-range dependency. To verify the effectiveness of the transformer, the LSTM-RNN is also considered as the baseline model.

*c) Prediction architecture:* To achieve multi-step prediction, there are two categories of prediction architectures, which are the iterative multi-step and direct multi-step prediction architecture. The advantage of the iterative multi-step method is that can achieve long-term prediction, however, this method is susceptible to accumulation errors. In contrast, the direct multi-step prediction architecture can exploit more information and has a high prediction accuracy [11]. Therefore, also these two architectures are used for baseline models.

To conduct the comparative analysis with the proposed methods, five baseline models are considered. Table I lists the input variables, prediction method, and prediction architecture of baseline models.

TABLE I
BASELINE MODELS

| Model | Input Variable | Prediction method | Architecture |
|---|---|---|---|
| M1 | $c$, $z$ | LSTM-RNN | Direct |
| M2 | $c$, $z$ | Transformer | Iterative |
| M3 | $c$, $z$ | LSTM-RNN | Iterative |
| M4 | $c$ | Transformer | Iterative |
| M5 | $c$ | LSTM-RNN | Iterative |

## IV. RESULTS AND DISCUSSION

This section presents battery capacity estimation by using EIS data based on the convolutional neural network (CNN) model, and the estimated capacity is used as the input of the capacity prediction model. For the capacity prediction part, the effectiveness of the transformer model and the impedance as the input variables are demonstrated, consequently, the results of different methods for battery capacity prediction are discussed.

### A. Verification of capacity estimation

The CNN model is trained by using the data from battery cell 25C01 to 25C04, where the features include 60 real part impedances and 60 imaginary part impedances.

The battery capacity estimation results of cells 25C05 to 25C08 are shown in Fig. 3, with the corresponding statistical errors listed in Table II. For all cells, the mean absolute error (MAE) and root mean square error (RMSE) is lower than 1.33 mAh and 1.15 mAh, respectively, which indicates that EIS data can sufficiently represent battery capacity degradation.

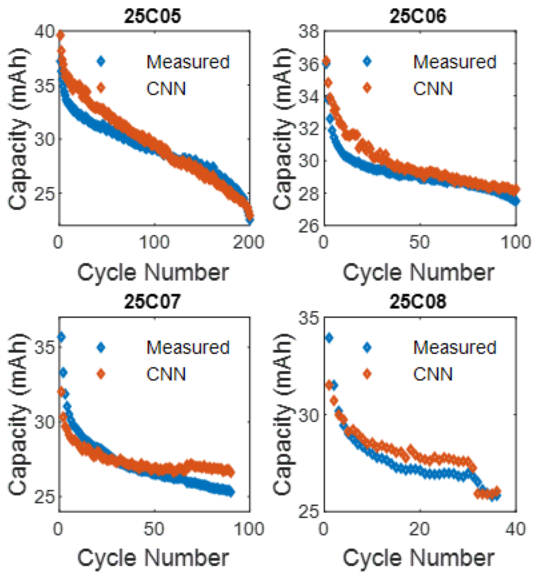


Fig. 3. Capacity estimation results of 25C05, 25C06, 25C07 and 25C08 based on CNN, where 60 real part impedances and 60 imaginary part impedances are used as the inputs of the CNN to automatically extract features.

TABLE II
CAPACITY ESTIMATION ERRORS IN MAH BASED ON CNN

| Cell Number | CNN MAE | CNN RMSE |
|---|---|---|
| 25C05 | 1.33 | 1.15 |
| 25C06 | 0.64 | 0.80 |
| 25C07 | 0.93 | 0.96 |
| 25C08 | 0.53 | 0.73 |

### B. Effectiveness of Transformer for long sequences

Compared with the LSTM-RNN, the transformer has the potential to capture long-range dependency, however, there are no published papers that study the effectiveness of the transformer model for the long data sequence as in the battery data set used in this paper. To demonstrate the influence of the length of input and output sequence on the accuracy of battery capacity prediction, different input and output time steps are applied for LSTM and transformer models and the accuracy of the different results is compared with each other. During the experiments, the actual capacity of 25C01 is used for training the model, and a part of the actual capacity of 25C05 is used for testing the model.

Fig. 4 presents the RMSE of the battery capacity prediction of the two models as a function of input and output steps. The capacity prediction error of the transformer model only slightly increases with the increase in output time steps, in contrast, the capacity prediction error of the LSTM-RNN model is significantly increasing with the increase of the output time steps. This shows that the transformer model indeed is more suitable for long-time step prediction than LSTM-RNN. Besides, as the input time step increases, there is a slight increase in capacity prediction error.

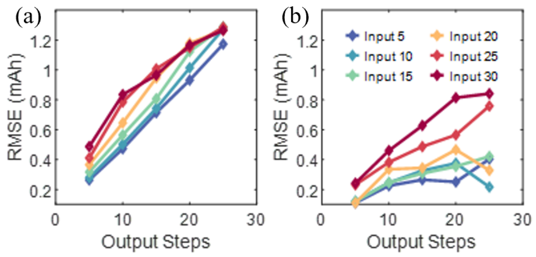


Fig. 4. The RMSE of battery capacity prediction of models for different input and output time steps. (a) LSTM-RNN model. (b) Transformer model.

According to Fig. 4 (b), when the length of input steps is 5, and the length of output steps is 15, the model achieves a balance between prediction length and prediction error. Compared with the model with the length of output steps of 20, the model with the length of output steps of 15 can achieve a more robust capacity prediction.

### C. Effectiveness of impedance for capacity prediction

The different feature sets in the EIS data are compared to verify the effectiveness of impedance as the input variable of battery capacity prediction models. During this experiment, two features are defined, named $F1$ and $F2$, the definition of them are $F1 = [C]$ and $F2 = [CZ]$, where $C$ presents the battery capacity sequence and $Z$ presents the imaginary part of the impedance sequence at the frequency of 2 Hz, which is highly correlated with battery capacity. The test model is the direct multi-step transformer prediction model, which is trained by using data from 2501-25C04, with the length of input and output steps of 5 cycles and 15 cycles, respectively. Due to the actual capacity being hard to measure in real applications, the input capacity sequence is the estimated capacity sequence, the impedance is measured by the EIS measurement device. This approach gives the method potential to use for online applications. To clearly show the prediction performance based on the two different features, the different prediction windows are shown in Fig. 5 and Fig. 6, in which part of battery capacity prediction results of 25C05-25C08 based on $F1$ and $F2$ are shown, respectively. Detailed experimental information is listed in Table III.

It is observed that all the cells with $F1$ and $F2$ can obtain capacity prediction results with relatively high accuracy. Compared with the results of using $F1$ given in Fig. 5, the results in Fig. 6 using $F2$ show a more accurate capacity prediction at all cycle ranges. Due to the lack of impedance information of $F1$, its accuracy is significantly lower than that of $F2$. Compared with other battery cells, the large prediction error of 25C08 is caused by the lower accuracy of capacity estimation results in Fig. 3. However, the prediction result of 25C08 when using $F2$ is more accurate than when using

TABLE III
EXPERIMENT DESCRIPTION FOR VERIFYING THE EFFECTIVENESS OF IMPEDANCE

| Item | Description |
|---|---|
| 1st Feature sets | $F1 = [C]$<br>$C$: Estimated capacity sequence |
| 2nd Feature sets | $F2 = [CZ]$<br>$C$: Estimated capacity sequence<br>$Z$: Measured Impedance sequence |
| Model | Direct Multi-step prediction transformer<br>Time steps: input: 5; output: 15<br>Trained by 25C01-25C04 |
| Prediction windows | 25C05: 6-20th, 56-70th, 101-115th, 156-170th<br>25C06: 6-20th, 26-40th, 56-70th, 86-100th<br>25C07: 6-20th, 26-40th, 56-70th<br>25C08: 6-20th, 16-30th |

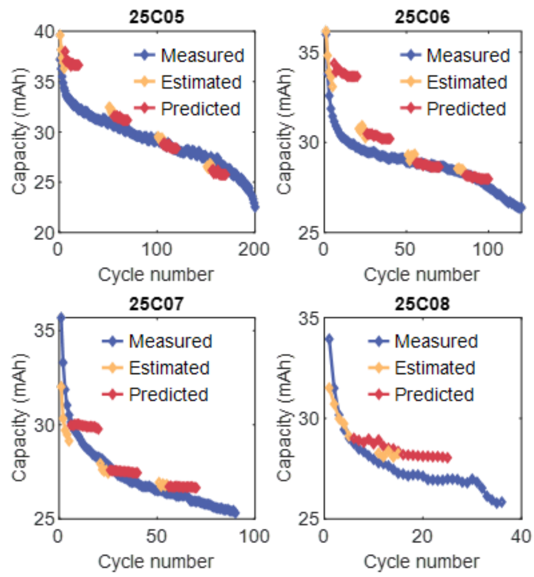


Fig. 5. The results of capacity prediction using $F1$ for different cells. The prediction windows for every cell are listed in Table III.

$F1$. It is clear therefore, that the availability of impedance information can improve the capacity prediction accuracy.

To show the capacity prediction error distribution of every point in a prediction window, the MAEs of every point in all prediction windows are calculated as,

$$MAE_{C_i} = \frac{1}{n-19} \sum_{j=1}^{n-19} |c_{ij} - \hat{c}_{ij}| \quad (2)$$

where $MAE_{C_i}$ is the MAE of $ith$ capacity prediction point, the maximum of $i$ is the direct capacity prediction length, which is 15. $j$ presents the $jth$ prediction window number, $n$ is the cycle number of capacity sequence, $n-19$ is the number of prediction windows, and $\hat{c}_{ij}$ is the predicted capacity at the $ith$ point of the $jth$ cycle. The results are shown in Table IV and Fig. 7.

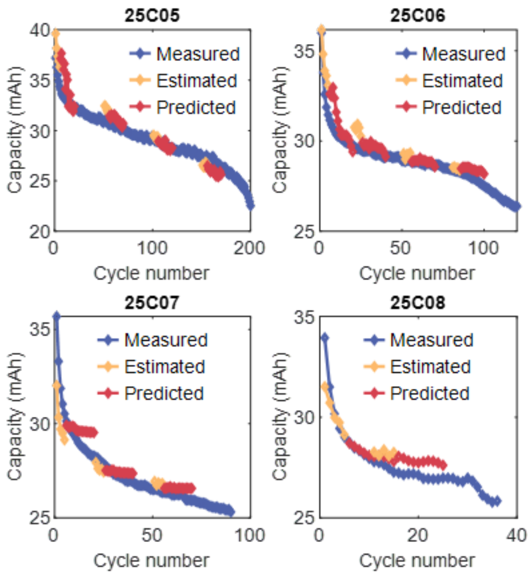


Fig. 6. The results of capacity prediction using $F2$ for different cells. The prediction windows for every cell are listed in Table III.

TABLE IV
CAPACITY PREDICTION ERRORS IN MAH BASED ON $F1$ AND $F2$

| Prediction Point | 25C05 | | 25C06 | | 25C07 | | 25C08 | |
|---|---|---|---|---|---|---|---|---|
| | F1 | F2 | F1 | F2 | F1 | F2 | F1 | F2 |
| 1st | 0.93 | 0.75 | 0.49 | 0.32 | 0.32 | 0.29 | 0.91 | 0.63 |
| 2nd | 0.85 | 0.72 | 0.50 | 0.33 | 0.30 | 0.27 | 1.04 | 0.63 |
| 3rd | 0.98 | 0.85 | 0.53 | 0.41 | 0.27 | 0.25 | 1.172 | 0.63 |
| 4th | 0.94 | 0.74 | 0.53 | 0.37 | 0.26 | 0.24 | 1.26 | 0.61 |
| 5th | 0.94 | 0.75 | 0.52 | 0.31 | 0.27 | 0.22 | 1.32 | 0.59 |
| 6th | 0.90 | 0.78 | 0.54 | 0.48 | 0.27 | 0.19 | 1.40 | 0.60 |
| 7th | 0.89 | 0.66 | 0.56 | 0.36 | 0.28 | 0.19 | 1.30 | 0.55 |
| 8th | 0.93 | 0.67 | 0.54 | 0.37 | 0.30 | 0.22 | 1.38 | 0.59 |
| 9th | 0.96 | 0.59 | 0.52 | 0.39 | 0.35 | 0.26 | 1.44 | 0.58 |
| 10th | 0.91 | 0.59 | 0.52 | 0.36 | 0.39 | 0.30 | 1.48 | 0.53 |
| 11th | 0.91 | 0.66 | 0.51 | 0.36 | 0.43 | 0.35 | 1.27 | 0.59 |
| 12th | 0.87 | 0.61 | 0.52 | 0.41 | 0.46 | 0.41 | 1.26 | 0.60 |
| 13th | 0.90 | 0.48 | 0.52 | 0.43 | 0.50 | 0.45 | 1.30 | 0.57 |
| 14th | 0.84 | 0.32 | 0.50 | 0.33 | 0.53 | 0.49 | 1.28 | 0.55 |
| 15th | 0.82 | 0.45 | 0.49 | 0.33 | 0.57 | 0.53 | 1.29 | 0.57 |

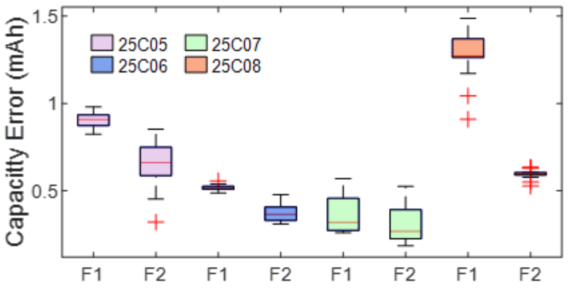


Fig. 7. The capacity prediction error distribution using $F1$ and $F2$ for different cells. On each box, the central mark indicates the median, and the bottom and top edge of the box represents the 25th and 75th percentiles, respectively. Excluding the outliers which are drawn separately using the '+' symbol, the whiskers extend at both end to the most extreme data points.

It can be observed that the capacity prediction accuracy using $F2$ is higher than using $F1$ for all cells, and its MAE is less than 0.75 mA. In contrast, the MAE of capacity prediction of 25C08 using $F1$ is higher than 1.3 mA. Therefore, the use of impedance data in this case improves the prediction accuracy with 30%.

### D. Results of different prediction methods

To show the effectiveness of the proposed method, which is the multivariate and direct multi-step prediction transformer model, the prediction results are shown in Fig. 8. The first prediction point is selected from all prediction windows, thus displaying the long-term prediction curve. It can be observed that the proposed model achieves accurate capacity prediction. For 25C08, the accuracy of capacity prediction is slightly improved compared to capacity estimation error. Improving the accuracy of capacity estimation is still crucial for accurate capacity prediction.

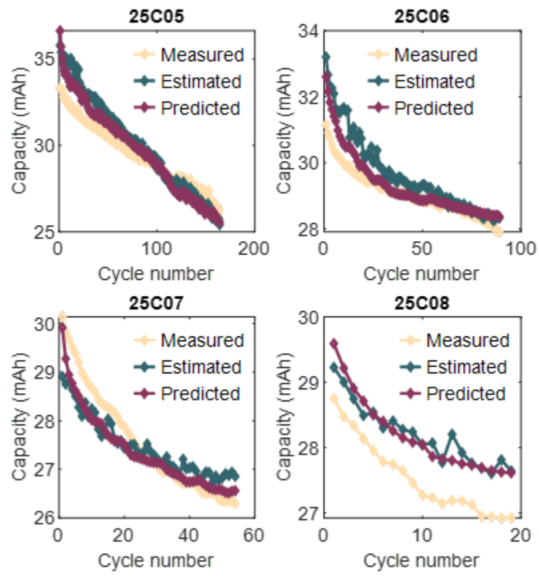


Fig. 8. The results of battery capacity prediction for different cells using the proposed method. The 1st prediction point is selected from all prediction windows.

To further compare the accuracy of capacity prediction among various methods, Table V lists the statistical errors of battery capacity prediction using the proposed method, five baseline methods, and a reference method [7], with the distribution of battery capacity prediction errors illustrated in Fig. 9. According to the results, the proposed model has the best performance. In terms of prediction architecture, the proposed method and M1 are more accurate than others, therefore, the prediction accuracy of direct multi-step prediction is higher than the iterative multi-step prediction method. From the aspects of the sequence prediction method, under the direct multi-step prediction architecture, the capacity prediction of the transformer model is more accurate than the results of LSTM-RNN, except for the 25C08, it is a trade-off result between the model generalization ability and accuracy for the low-consistency cells, but no obvious improvement is observed when using the transformer model under the iterative multi-step prediction architecture. Finally, the prediction errors can be further reduced by using a multivariate model rather than using a univariate model.

TABLE V
CAPACITY ESTIMATION ERRORS IN MAH BASED ON DIFFERENT METHODS

| Cell Number | MAE | | | | | | |
|---|---|---|---|---|---|---|---|
| | **Proposed** | **M1** | **M2** | **M3** | **M4** | **M5** | **Ref [7]** |
| 25C05 | 0.32 | 1.54 | 1.36 | 1.26 | 3.00 | 3.59 | 0.69 |
| 25C06 | 0.08 | 0.65 | 1.90 | 0.64 | 2.10 | 1.26 | 1.91 |
| 25C07 | 0.29 | 0.36 | 0.94 | 0.78 | 0.43 | 1.64 | 1.15 |
| 25C08 | 0.64 | 0.33 | 0.84 | 1.01 | 0.76 | 1.22 | 1.74 |

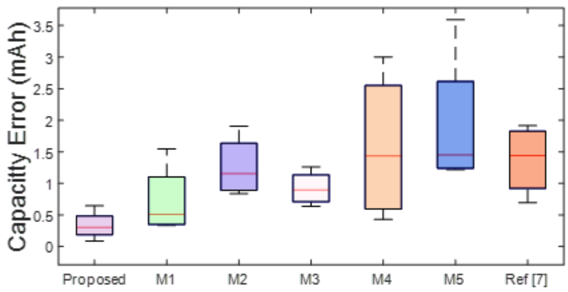


Fig. 9. The capacity prediction errors distribution of different methods for 25C05-25C08 cells. M1-M5 are the five baseline methods listed in Table I.

To demonstrate the performance of the proposed model in early battery capacity prediction, five published methods are investigated. It can be observed from Fig. 10, the starting prediction point of four published papers for battery capacity is after 50 cycles, so these papers cannot achieve early battery capacity prediction [5] [4] [6] [12]. Besides, the length of the battery capacity prediction window of the proposed model is greater than that of another published direct multi-step prediction model [7]. Therefore, compared to published papers, the proposed method can achieve earlier capacity prediction.

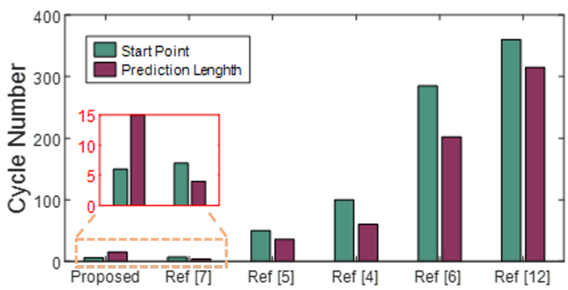


Fig. 10. Results of start points and prediction length of the proposed and several published methods for capacity prediction.

## V. CONCLUSION

A multivariate and direct multi-step prediction transformer model is proposed for early battery capacity prediction, based on EIS and battery capacity data. Since the actual battery capacity is difficult to determine in the real battery applications, first a CNN model is used for battery capacity estimation based on broadband EIS data. The estimated capacity sequence is subsequently used together with the EIS data as the input sequence for the multivariate and direct multi-step prediction transformer model for capacity prediction. When impedance data is used as input of the transformer model, the capacity prediction errors are reduced by around 30% with respect to the case where only the estimated capacity sequence is used as input. Moreover, compared with five baseline models and a published model, the proposed model has the best performance with an MAE of less than 0.64 mA for four test cells. Finally, compared with five published methods, the proposed model can indeed achieve earlier capacity prediction, with only 5 cycles of data needed for a 15-cycle prediction.

The performance of the proposed model needs to be further verified on different operation conditions of the battery system, such as different temperatures, and for different battery chemistries.

## REFERENCES


[1] Z. Ning, Z. Deng, J. Li, H. Liu, and W. Guo, "Co-estimation of state of charge and state of health for 48 v battery system based on cubature kalman filter and h-infinity," *Journal of Energy Storage*, vol. 56, p. 106052, 2022.

[2] Z. Deng, L. Xu, H. Liu, X. Hu, Z. Duan, and Y. Xu, "Prognostics of battery capacity based on charging data and data-driven methods for on-road vehicles," *Applied Energy*, vol. 339, p. 120954, 2023.

[3] R. Eskandari, P. Venugopal, and G. Rietveld, "Advanced battery management systems with integrated battery electronics," in *2022 IEEE 20th International Power Electronics and Motion Control Conference (PEMC)*, pp. 55–61, IEEE, 2022.

[4] X. Gu, K. See, P. Li, K. Shan, Y. Wang, L. Zhao, K. C. Lim, and N. Zhang, "A novel state-of-health estimation for the lithium-ion battery using a convolutional neural network and transformer model," *Energy*, vol. 262, p. 125501, 2023.

[5] J. Yu, "State of health prediction of lithium-ion batteries: Multiscale logic regression and gaussian process regression ensemble," *Reliability Engineering & System Safety*, vol. 174, pp. 82–95, 2018.

[6] Y. Zhang, R. Xiong, H. He, and M. G. Pecht, "Long short-term memory recurrent neural network for remaining useful life prediction of lithium-ion batteries," *IEEE Transactions on Vehicular Technology*, vol. 67, no. 7, pp. 5695–5705, 2018.

[7] M. Zhang, T. Hu, L. Wu, G. Kang, and Y. Guan, "A method for capacity estimation of lithium-ion batteries based on adaptive time-shifting broad learning system," *Energy*, vol. 231, p. 120959, 2021.

[8] H. Zhou, S. Zhang, J. Peng, S. Zhang, J. Li, H. Xiong, and W. Zhang, "Informer: Beyond efficient transformer for long sequence time-series forecasting," in *Proceedings of the AAAI conference on artificial intelligence*, vol. 35, pp. 11106–11115, 2021.

[9] A. Zeng, M. Chen, L. Zhang, and Q. Xu, "Are transformers effective for time series forecasting?," *arXiv preprint arXiv:2205.13504*, 2022.

[10] Y. Zhang, Q. Tang, Y. Zhang, J. Wang, U. Stimming, and A. A. Lee, "Identifying degradation patterns of lithium ion batteries from impedance spectroscopy using machine learning," *Nature communications*, vol. 11, no. 1, p. 1706, 2020.

[11] X. Hu, L. Xu, X. Lin, and M. Pecht, "Battery lifetime prognostics," *Joule*, vol. 4, no. 2, pp. 310–346, 2020.

[12] X. Li, L. Zhang, Z. Wang, and P. Dong, "Remaining useful life prediction for lithium-ion batteries based on a hybrid model combining the long short-term memory and elman neural networks," *Journal of Energy Storage*, vol. 21, pp. 510–518, 2019.